Cell Stem Cell
Article

Histone Deacetylase Inhibition Elicits an Evolutionarily Conserved Self-Renewal Program in Embryonic Stem Cells

Carol B. Ware,[1,2,*] Linlin Wang,[1,3] Brigham H. Mecham,[7] Lanlan Shen,[11] Angelique M. Nelson,[1,2] Merav Bar,[9] Deepak A. Lamba,[1,6] Derek S. Dauphin,[3] Brian Buckingham,[4] Bardia Askari,[8] Raymond Lim,[10] Muneesh Tewari,[1,9] Stanley M. Gartler,[5,7] Jean-Pierre Issa,[11] Paul Pavlidis,[10] Zhijun Duan,[1,3] and C. Anthony Blau[1,3,7,*]

[1]Institute for Stem Cell and Regenerative Medicine
[2]Department of Comparative Medicine
[3]Department of Medicine/Hematology
[4]Medical Scientist Training Program
[5]Department of Medicine/Medical Genetics
[6]Department of Biological Structure
[7]Department of Genome Sciences
[8]Department of Pathology
University of Washington, Seattle, WA 98195, USA
[9]Fred Hutchinson Cancer Research Center, Seattle, WA 98109, USA
[10]Department of Psychiatry and Centre for High-Throughput Biology, University of British Columbia, Vancouver, BC V6T 1Z4, Canada
[11]MD Anderson Cancer Center, Houston, TX 77030, USA
*Correspondence: cware@u.washington.edu (C.B.W.), tblau@u.washington.edu (C.A.B.)
DOI 10.1016/j.stem.2009.03.001

SUMMARY

Recent evidence indicates that mouse and human embryonic stem cells (ESCs) are fixed at different developmental stages, with the former positioned earlier. We show that a narrow concentration of the naturally occurring short-chain fatty acid, sodium butyrate, supports the extensive self-renewal of mouse and human ESCs, while promoting their convergence toward an intermediate stem cell state. In response to butyrate, human ESCs regress to an earlier developmental stage characterized by a gene expression profile resembling that of mouse ESCs, preventing precocious *Xist* expression while retaining the ability to form complex teratomas in vivo. Other histone deacetylase inhibitors (HDACi) also support human ESC self-renewal. Our results indicate that HDACi can promote ESC self-renewal across species, and demonstrate that ESCs can toggle between alternative states in response to environmental factors.

INTRODUCTION

Embryonic stem cells (ESCs) might be regarded as a tissue culture artifact (Smith, 2001), plucked from the preimplantation blastocyst and supported using culture conditions bearing little resemblance to conditions in vivo. Even leukemia inhibitory factor (LIF), the quintessential extracellular regulator of mouse ESC self-renewal, is not required for development other than for implantation (Stewart et al., 1992; Ware et al., 1995). Nowhere is the lack of a physiological context for ESCs more pressing than in attempts to define their cellular identity, also known as the "stem cell state" (Buszczak and Spradling, 2006). One definition of the ESC state is the epigenetic state that endows ESCs with the unique option to self-renew or to differentiate into any cell type in the body.

It has been proposed that an epigenetic event may be rate-limiting in the derivation of new ESC lines (Smith, 2001; Thomson et al., 1998) and may further operate in selecting for ESCs that adapt to standard culture conditions. An epigenomic bottleneck might similarly explain the inefficiency inherent in generating new ES-like cells—induced pluripotent stem (iPS) cells (Takahashi and Yamanaka, 2006; Nakagawa et al., 2007; Park et al., 2007; Takahashi et al., 2007; Yu et al., 2007) and epiblast stem cells (EpiSCs) (Brons et al., 2007; Tesar et al., 2007). Stated differently, our current understanding of the ESC state may be influenced by the manner in which ESCs are derived and maintained. Consistent with this interpretation was the recent demonstration that the efficiency of iPS cell formation is enhanced upon addition of valproic acid, an inhibitor of histone deacetylases, to the culture medium (Huangfu et al., 2008).

Despite their uncertain in vivo corollary, studies using in vitro cultured ESCs have enhanced our understanding of how stem cells work (Bernstein et al., 2006; Ivanova et al., 2006; Chambers et al., 2007; Ying et al., 2008). To self-renew, ESCs must stably propagate their epigenetic patterns through cell division. Fundamental differences exist in the mechanisms by which mouse ESCs (mESCs) and human ESCs (hESCs) self-renew. mESCs respond to LIF-triggered activation of STAT3, whereas hESC do not (Dahéron et al., 2004). hESCs respond to superphysiological levels of bFGF (Levenstein et al., 2006) and to Activin A (Vallier et al., 2005; Xiao et al., 2006) to maintain pluripotency. The differences in culture conditions for mESCs and hESCs might be explained by the recent finding that mouse and human ESCs are not developmental equals, with the former

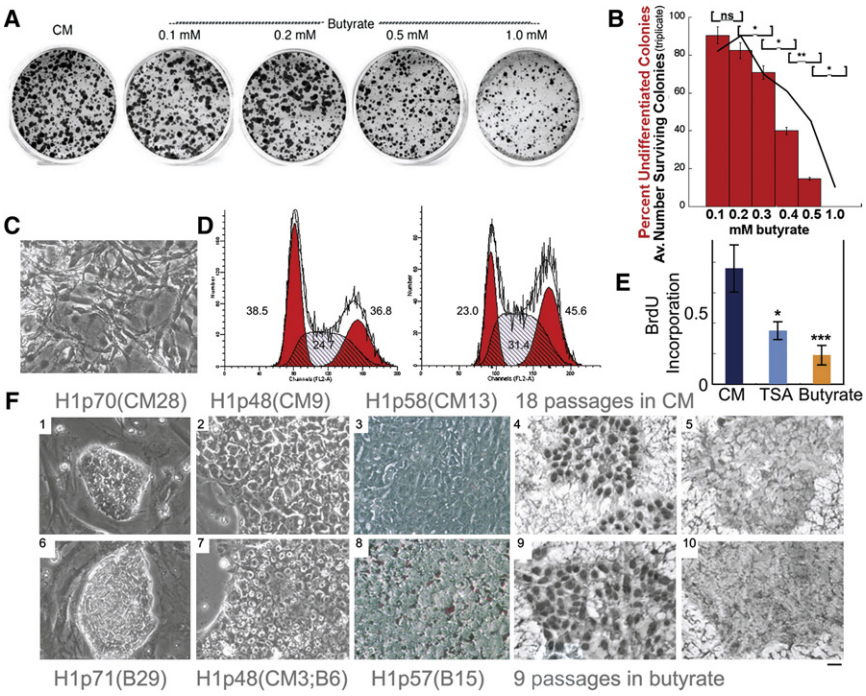

Figure 1. Butyrate Supports the Self-Renewal of H1 Cells

(A) H1 cells acclimated to growth in CM (which contains 2 ng/ml FGF2-see methods) were cultured on Matrigel-coated 35 mm dishes for 4 days in conditioned medium (CM) or in hESM (which lacks conditioning or FGF2) at the indicated concentrations of butyrate. Undifferentiated colonies were scored based on alkaline phosphatase staining.

(B) Quantitative results from a repeat of the experiment shown in (A) performed in triplicate. Black line indicates numbers of colonies per dish. *$p < 0.05$; **$p < 0.01$. Red bars indicate percentages of alkaline phosphatase-positive colonies. Error bars denote standard error of the mean.

(C) Appearance of differentiated cells that appear transiently after switching from CM to butyrate for two passages.

(D) Cell-cycle profiles of H1 cells cultured in CM (left) versus butyrate (right). Numbers indicate percentages of cells in G1/S/G2. Note increases in percentages of cells in S and G2 in the butyrate cultures. These findings are representative of two independent experiments.

(E) Bromodeoxyuridine (BrdU) incorporation in H1 cells cultured in CM, trichostatin A (TSA) (10 nM) (*$p < 0.05$; CM versus TSA), and butyrate (0.2 mM) (***$p < 0.001$; CM versus butyrate). Error bars denote standard error of the mean.

(F) Morphology of H1 cells cultured in CM (F1–F5) or butyrate (F6–F10). (F1) and (F6), on feeders; (F2)–(F5) and (F7)–(F10), on Matrigel; (F3) and (F8), oil red O-stained; (F4) and (F9), Pou5F1 (Oct4)-stained; and (F5) and (F10), secondary control antibody staining companions to Pou5f1 staining. Note that in (F1), H1p70(CM28) is 70 passages total, the last 28 of which were without feeder in CM; in (F6), H1p71(B29) is 71 passages total, the last 29 of which were in butyrate; and for (F7), H1p48(CM3;B6) is 48 passages total, and within the last 9 passages, the first 3 were without feeder in CM and the final 6 passages were in butyrate. This format is followed for all subsequent figures. The size bar indicates 38 μm in (C) and (F1), and 6 and 15 μm in (F2)–(F5) and (F7)–(F10), respectively.

representing an earlier developmental stage (Brons et al., 2007; Tesar et al., 2007).

ESCs and cancer cells employ overlapping signaling networks (Dreesen and Brivanlou, 2007; Wong et al., 2008; Ben-Porath et al., 2008), raising the possibility that understanding self-renewal in ESCs might bring new insights to cancer therapy. Recently, histone deacetylase (HDAC) inhibitors (HDACi) have emerged as an important new class of anticancer drug (Xu et al., 2007). Here, we show that both naturally occurring and synthetic HDACi promote ESC self-renewal using defined, serum-free culture conditions. HDACi induce a shift in the gene expression profiles of human and mouse ESCs toward a state intermediate between ESCs and EpiSCs. Our results define an alternative ESC state and point to the existence of an evolutionarily conserved self-renewal program.

RESULTS

A Narrow Concentration of Sodium Butyrate Maintains hESCs in an Undifferentiated State

H1 cells cultured on Matrigel-coated dishes were switched from standard culture conditions (conditioned medium that includes FGF2; CM) to feeder-free culture in hESC medium (hESM) without feeder conditioning with a range of sodium butyrate concentrations. hESM contains a proprietary serum replacer (KSR, Invitrogen), but lacks FGF2 or other growth factors. We found that the butyrate concentrations used in most publications (>1.0 mM; Boffa et al., 1978) were toxic in hESC cultures and did not allow for sustained growth (Figures 1A and 1B). However lower butyrate concentrations (0.2 to 0.3 mM) induced a transient wave of differentiation (Figure 1C), followed by the outgrowth of approximately 50% of the original cell population as undifferentiated hESC that could be maintained in culture indefinitely (at least 33 passages over 7 months). ESCs are thought to lack a G1 checkpoint (Savatier et al., 1994; Becker et al., 2007). H1 cells cultured in hESM with 0.2 mM butyrate accumulated cells in S and G2, consistent with a relative G2/M block (Figure 1D). A similar accumulation of cells in G2/M was recently reported for γ-aminobutyric acid (Andäng et al., 2008). Butyrate-converted hESC divided at about one-quarter the rate of cells cultured according to standard conditions as measured by BrdU incorporation (Figure 1E). Notably, 0.2 mM butyrate was not associated with a significant induction of p21 by real-time quantitative PCR (qPCR; data not shown). Once acclimated, butyrate-treated cells formed tightly clustered colonies that adhered firmly to Matrigel and lacked the small percentage of differentiated cells that normally accompany H1 cells cultured in CM (Figure 1F). Butyrate also induced the appearance of lipid droplets as determined by oil red O staining (Figure 1F, panel 8).

We confirmed the undifferentiated features of butyrate-converted H1 cells by assessing a series of ESC-specific markers and by measuring telomerase activity (Figure 1F9 and Figure S1 available online). In total, six different hESC lines (H1

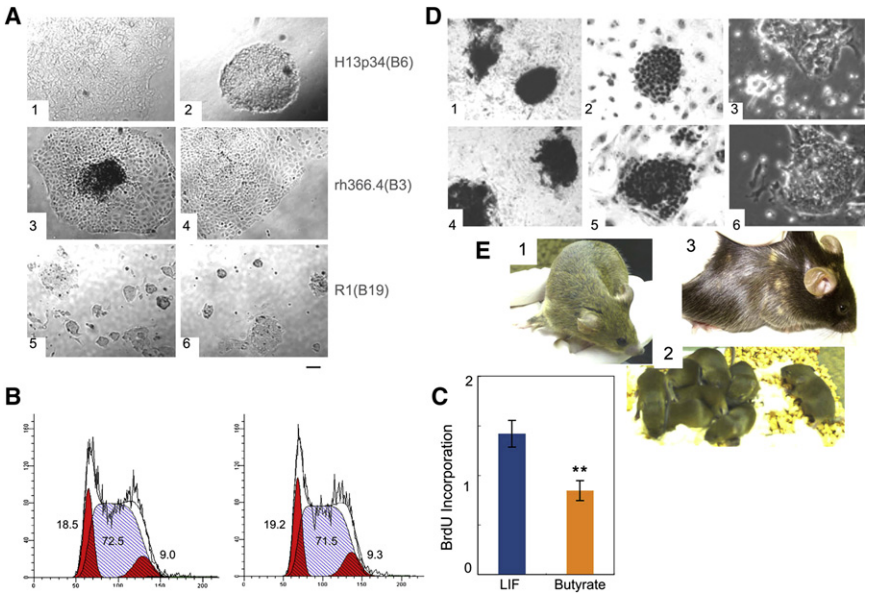

Figure 2. Butyrate Supports ESC Self-Renewal Across Species

(A) H13 cells ([A1] in CM and [A2] in butyrate), rh366.4 rhesus ESCs ([A3] in CM and [A4] in butyrate), R1 mouse ESCs ([A5] in LIF and [A6] in butyrate).

(B) Cell-cycle profile of R1 cells cultured in LIF (left) or butyrate (right).

(C) BrdU uptake in R1 cells cultured in LIF versus butyrate. **p < 0.01. Error bars denote standard error of the mean.

(D) Alkaline phosphatase staining (D1 and D4), Pou5f1 (Oct4) staining (D2 and D5), and phase-contrast microscopy (D3 and D6) of R1 cells cultured in LIF (D1–D3) or 0.2 mM butyrate (D4–D6).

(E) Chimeric mouse generated from R1 ESCs cultured for three passages in butyrate plus LIF on feeders (E1) and its progeny (E2), indicating 100% germ line transmission (note: all are brown). Chimeric mouse from mEpiSC line no. 5, a gift from Paul Tesar and Ron McKay (Tesar et al., 2007), cultured for 18 passages on feeders with the addition of butyrate for the last 8 passages (panel 3). The size bar indicates 38 μm for (A) and (D).

[National Institutes of Health designation WA01], H9 [WA09], H13 [WA13], BG02, BG03, hSF6 [UC06]) and a rhesus ESC line (rh366.4) were converted to butyrate-dependent, MEF/CM-independent culture conditions in hESM supplemented with 0.2 to 0.3 mM sodium butyrate, but lacking FGF2 or other growth factors (Figure 2A; Table S1). We observed differences among hESC lines in their responses to butyrate. BG03 cells were readily converted to butyrate, with little evidence of differentiation. H1 cells were more fastidious, requiring dense plating prior to butyrate exposure and 1:1 passaging (for at least 2 passages) after butyrate addition. The concomitant presence of feeder cells eased the conversion of some (H9), but not all (H1, BG02, and BG03), hESC lines. The emergence of karyotypic abnormalities, common in hESC cultures (Denning et al., 2006; Ware et al., 2006; Baker et al., 2007), occurred in butyrate cultures at rates similar to CM (Table S1 and Figure S2). Although trisomy 17 is a common abnormality in hESC cultures (Baker et al., 2007), we have not observed trisomy 17 in butyrate-treated hESCs.

Notwithstanding the well-established differences between the self-renewal programs of mouse and human ESCs, butyrate also promoted the extensive self-renewal of a mESC line (R1) (Figures 2A and 2D). mESCs cultured in butyrate-containing medium without LIF (see the Experimental Procedures) adopted a very similar appearance to mESCs cultured in LIF. In both conditions, scattered differentiated cells at the colony periphery surrounded undifferentiated cells located centrally. In mESC, butyrate slowed the rate of cell division without perturbing the cell cycle (Figures 2B and 2C). Based on the resulting hypothesis that butyrate-induced ESC self-renewal arises from a common, evolutionarily conserved mechanism, we predicted that butyrate-induced self-renewal of mESCs could occur in the absence of LIF signaling. Confirming this prediction, we showed that mESCs lacking either the LIF receptor specific subunit or its shared gp130 partner could be converted to butyrate culture conditions (Figure S3).

Differentiation Potential of Butyrate-Treated ESCs

Teratomas generated by butyrate-converted hESCs were complex, containing prominent carrot-shaped cells with rod-shaped cytoplasmic granules, consistent with melanin containing pigmented ectoderm (both in H1 and BG02 cells), while the CM exposed counterparts rarely contained identifiable melanin (Figure S4). To more rigorously evaluate the differentiation potential of ESCs exposed to butyrate, we used mESCs. We added butyrate to mESC (R1) cultured on feeders supplemented with LIF for three passages, and these cells contributed to multiple tissues in two high-level chimeras, including the germline (Figures 2E1 and 2E2). In addition, two different gene-targeted mESC clones that had not previously contributed to coat-color chimerism using standard culture conditions were able to generate high-level chimeras when butyrate was added to MEF-containing cultures (Table S2). These clones did not contribute to the germline, likely due to pre-existing abnormalities. Additionally, we were able to derive a new C57BL/6 mESC line in the presence of butyrate on MEFs that contributed extensively to coat-color chimerism (Table S2). While mESCs cultured in butyrate in MEF-free conditions did not generate chimeras (data not shown), our results demonstrate that adding butyrate to MEF-containing cultures can maintain and may even augment the ability of mESCs to contribute to various tissues in vivo.

Butyrate-Induced Transcriptional Response in hESCs

We used whole-genome arrays to compare the transcriptomes of feeder-free H1 cells cultured according to three conditions (each in triplicate): (1) standard culture conditions (CM with 2 ng/ml bFGF on Matrigel; H1p48[CM9]) (Group A); (2) cells from the same pool as group A converted to butyrate for six passages (hESM with 0.2 mM butyrate on Matrigel; H1p48[CM3;B6]) (group B); and (3) cells from the same pool as group B cultured in butyrate for four passages, then reverted back to standard culture conditions for three passages

(H1p49[CM3;B4;CM3]) (group C). Groups A and B and groups B and C were directly compared on Agilent arrays. A supervised cluster analysis readily distinguished the three groups (Figure S5). Butyrate significantly regulated 479 genes: 250 were upregulated, and 229 were downregulated (https://depts.washington.edu/iscrm/GS_data/gsdata.html). The large number of downregulated transcripts is consistent with a recognized but poorly understood role for butyrate in gene repression (Rada-Iglesias et al., 2007). The top 15 upregulated and downregulated genes are shown in Table S3. qPCR confirmed the differential regulation of all 14 representative genes tested (Figure S6A). Butyrate strongly induced several embryonic- and germ-cell-associated transcripts including *Dppa5* (*Esg1*), *Piwil2*, *Bnc1*, *Lrrc8e*, *Mbd3*, and *Ecat8* while downregulating *Tcf3* and *Gata6* (Table S4). *Dppa5*, *Piwil2*, *Ecat8*, *Ddx25*, and *Ddx43* all encode RNA-binding proteins, while *Mbd3* is a part of the *nu*cleosome *r*emodeling and histone *d*eacetylation (NuRD) corepressor complex associated with cell-fate decisions and pluripotency (Kaji et al., 2007). *Dppa5* and *Ddx43*/*HAGE*, the first and second most strongly induced genes, are spaced 60 kilobases apart on chromosome 6, and *Ecat1* is positioned between them. While *Ecat1* was not represented on the microarray, we found that it is also induced by butyrate (Figures 6B and 6C).

Several members of the canonical Wnt signaling pathway were downregulated by butyrate, including *Wnt3*, *Tcf3*, *Frzb*, and *Sfrp2*, as were β-catenin targets *Sp5* (Weidinger et al., 2000), *Gad1* (Li et al., 2004), *Fst* (Yao et al., 2004), *Lefty1* (Tabibzadeh and Hemmati-Brivanlou, 2006), *Pitx2* (Zirn et al., 2006), and *Id2* (Willert et al., 2002). An increase in *Inhba* (INHBA homodimerizes to form ACTIVIN A) and reduced expression of *Lefty1* and *Fst* indicate that the TGFβ pathway may be recruited to maintain self-renewal of butyrate-treated hESCs (Vallier et al., 2005; Xiao et al., 2006; Eiselleova et al., 2008). Butyrate treatment also resulted in downregulation of *Tcf3*, a repressor of *Nanog* in mESCs (Pereira et al., 2006; Yi et al., 2008). While butyrate did not induce a significant change in *Nanog* levels, we found *Nanog* to be consistently (albeit subtly) elevated in hESCs cultured in butyrate relative to CM (Figure S1B). NANOG stabilizes ESCs in culture, underpinning the epigenetic erasure unique to pluripotent and germ cells (Chambers et al., 2007). A subtle rise in *Nanog* may reflect the absence of differentiating cells in butyrate-acclimated cultures.

Withdrawal from feeder cells was not necessary to elicit the butyrate transcriptional program, since *Dppa5*, *Ecat1*, and *Piwil2* were all induced in H13 cells three passages after adding butyrate to feeder-containing cultures (Figure S6B). Approximately 85% of genes that were differentially expressed in response to butyrate (group B versus group A) (Figure 3A) returned promptly to near-baseline levels after reverting back to standard culture conditions (group C versus group A) (Figure 3B). Conversely, some butyrate-responsive genes remained persistently altered following three passages in CM (Figure 3B and Table S4). Persistently induced genes included *Dppa5*, *Ddx43*/*HAGE*, and *Ecat1* (Figure S6C). The basis for this persistent effect on the expression of some genes long after butyrate withdrawal suggests the presence of distinct mechanisms for regulating these genes. A significant overlap in butyrate-regulated genes occurred between H1 cells and a second hESC line, BG02 (Figure 3C). The similar transcriptional responses between H1 and BG02 were highly significant ($p < 0.0001$).

A Distinct Transcriptional Response to Butyrate in mESCs

We also compared the transcriptional profiles of mESCs cultured according to our standard MEF-free culture conditions (the medium was identical to hESM, except that 20% fetal bovine serum substitutes for serum replacer, plus the addition of LIF) versus butyrate (using the same medium without LIF). Supervised cluster analysis distinguished the two groups (Figure S7). Strikingly, there was very little overlap between the lists of butyrate-regulated genes in mESCs and hESCs (https://depts.washington.edu/iscrm/GS_data/gsdata.html). Even genes that were dramatically induced by butyrate in hESCs (*Dppa5*, *Ddx43*/*HAGE*, and *Piwil2*) were unchanged or even very modestly downregulated (in the case of the *Piwil2* homolog *Mili*) in mESCs.

Butyrate Induces the Convergence of hESCs and mESCs toward a Common Developmental Intermediate

Two recent reports described the derivation of epiblast stem cells (EpiSCs) from postimplantation mouse blastocysts and that EpiSCs more closely resemble hESCs than do mESCs (Brons et al., 2007; Tesar et al., 2007). We reasoned that the contrasting effects of butyrate on the transcriptional profiles of hESCs versus mESCs might be reconciled if butyrate brought both hESCs and mESCs nearer one another toward a developmental stage intermediate between mESCs and mouse EpiSCs (mEpiSCs). To test this hypothesis, we correlated butyrate-induced transcriptional responses in hESCs and mESCs with the published transcriptional profiles of mESCs versus mEpiSCs. Figures 3D–3F present identical scattergrams (black dots) comparing the relative levels of gene expression from published mRNA microarrays of mESCs (x axis) versus EpiSCs (y axis) (Tesar et al., 2007). In Figures 3D and 3E, mouse homologs of genes that are significantly induced or repressed by butyrate in H1 and BG02 cells are overlaid as red or green dots, respectively. Note that butyrate-induced genes in hESCs (red) are homologous to genes that tend to be more highly expressed in mESCs and localize nearer the x axis, whereas homologs of butyrate-repressed transcripts (green) tend to be more abundant in EpiSCs. This correlation is consistent with the interpretation that butyrate shifts the transcriptional program of hESCs away from EpiSCs and toward mESCs. Strikingly, Figure 3F shows the opposite pattern in the mESC line R1: genes that are significantly induced by butyrate in mESCs (red) tend to be more highly expressed in EpiSCs, whereas butyrate-repressed genes tend to be expressed at higher levels in mESCs. Figure 4 shows results for ESC-associated genes, comparing butyrate responses in hESCs with the relative expression levels of their mouse homologs in mESCs versus EpiSCs. These patterns were highly significant and support the initial observation that mEpiSCs and hESCs equate to a similar embryonic stage with mESCs positioned earlier (Brons et al., 2007; Tesar et al., 2007) and that butyrate advances mESCs and retracts hESCs toward a developmental state intermediate between mESCs (inner cell mass, ICM) and hESCs (epiblast).

To further examine the hypothesis that butyrate exposure pulls hESCs and mEpiSCs backward toward an earlier developmental

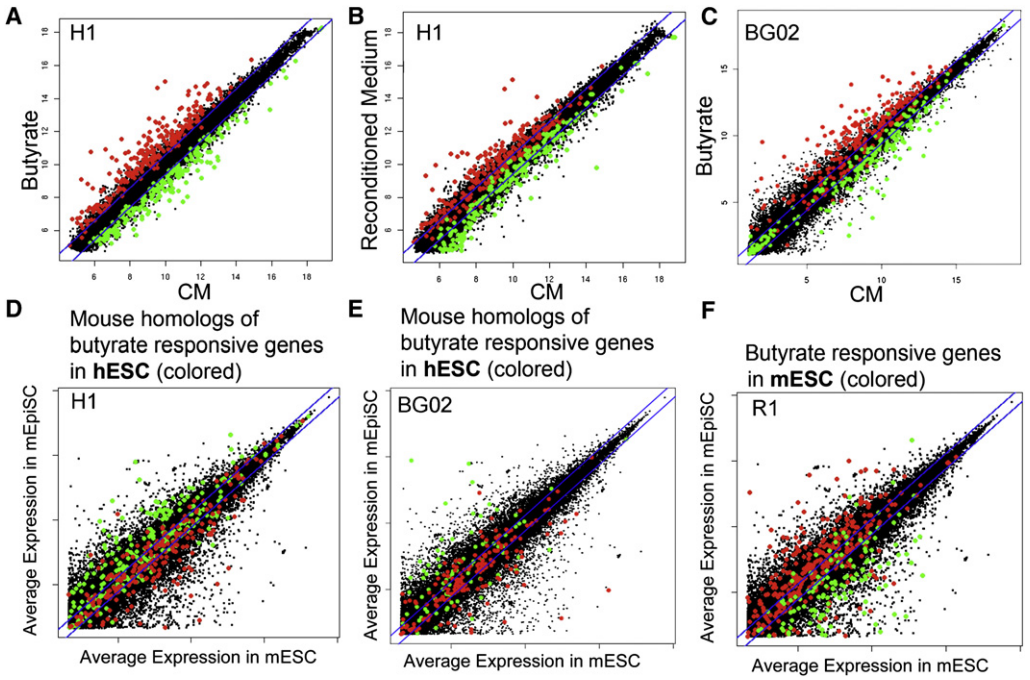

Figure 3. Transcriptional Responses to Butyrate in Human and Mouse ESCs

Colored dots depict genes that are significantly upregulated (red) or downregulated (green) in response to butyrate in the hESC lines H1 (A–D) and BG02 (E), and the mESC line R1 (F).

(A) Scatter plot depicting the transcriptional response of H1 cells cultured for six passages in butyrate versus H1 cells maintained in CM (see text for details).

(B) Reversion toward the original pattern of expression after returning butyrate-treated H1 cells back to CM for three passages ("Reconditioned Medium").

(C) Scatter plot depicting the transcriptional response to butyrate in BG02 cells (black dots), with red and green dots identifying those genes that were butyrate-regulated in H1 cells, to highlight genes that were coordinately regulated in both hESC lines.

(D–F) Scatter plots (in black) depicting average expression levels in mEpiSCs versus mESC (from Tesar et al., 2007; identical for all three panels). (D) and (E) overlay butyrate responsive homologous genes in H1 and BG02 cells, respectively. Colored dots indicate homologous genes in the hESC lines that were significantly upregulated (red) or downregulated (green) in response to butyrate. (F) overlays butyrate-responsive genes in mESCs. Colored dot overlays indicate genes in mESCs (R1 cells) that were significantly upregulated (red) or downregulated (green) in response to butyrate. Note that butyrate pulls the gene expression profile of hESCs toward mESCs (x axis) and away from mEpiSCs (y axis) while pushing mESCs toward EpiSCs; thus, the relative orientation of red and green dots between (D) and (E) versus (F) is reversed. Two sample t tests assuming equal variance indicate that these changes are highly significant ([D], $t = -9.921$; [E]: $t = -4.88$; [F], $t = 11.139$; $p < 0.001$; see Supplemental Experimental Procedures).

stage, we performed additional studies. Some female hESC lines harbor an inactive X chromosome, reflected in the presence of Xist bodies (International Stem Cell Initiative et al., 2007; Hall et al., 2008). *Xist* expression is abundant in later passage H9 cells (p77) cultured on feeders (92 of 104 cells scored [88.5%]), but was undetectable in H9 cells cultured for 31 passages in hESM plus butyrate (0 of 108 cells scored [0%]) (Figure 5, panels 1–7). However *Xist* was expressed in butyrate-treated H9 cells after 21 days of differentiation (Figure 5, panels 8–11). We also found that butyrate-treated hESCs differentiated more gradually than hESCs cultured in CM, as evidenced by a slower decline in 302 family miRNAs (Figure 6A) and by a delay in directed differentiation toward retinal neurons (Lamba et al., 2006; Figure 6B). This butyrate-induced differentiation delay was reversed in part by returning butyrate-exposed cells to CM for three passages prior to differentiation (Figure 6B).

We also tested butyrate's effect on mEpiSCs (Tesar et al., 2007; Figure S8). Hallmark functional differences between mESCs and mEpiSCs include the latter's nonresponsiveness to LIF and markedly reduced ability to generate chimeras (Brons et al., 2007; Tesar et al., 2007). While butyrate did not induce LIF dependency nor feeder independency in mEpiSCs (data not shown), its presence did allow an mEpiSC line provided by Tesar and McKay to generate a single coat-color chimera in 14 pups (48 blastocysts injected; Figure 2E3).

Butyrate Induces H3K9 Acetylation and CpG Demethylation at the *Dppa5* Promoter

We examined the epigenetic responses of a number of butyrate-regulated genes using chromatin immunoprecipitation (ChIP) assays. The promoters of some (*Dppa5*, *Ddx43*, and *Rcn3*), but not all (*Cxcl5*), butyrate-induced genes displayed a corresponding rise in H3K9 acetylation, whereas repressed genes showed little change (*Dusp6* and *Ier5*) or a decline (*Sp5*) in H3K9 acetylation (Figure 7A). Bisulfite sequencing of the *Dppa5* promoter showed a striking decline in DNA methylation in H1 cells treated with butyrate, and a very similar response occurred in BG02 cells (Figure 7B). For both hESC lines, the residual methylation in butyrate-treated cells was concentrated among a few clones, consistent with a butyrate-induced inhibition of *Dppa5* methylation following DNA replication. Serial monitoring of the *Dppa5* promoter at various time points following butyrate exposure

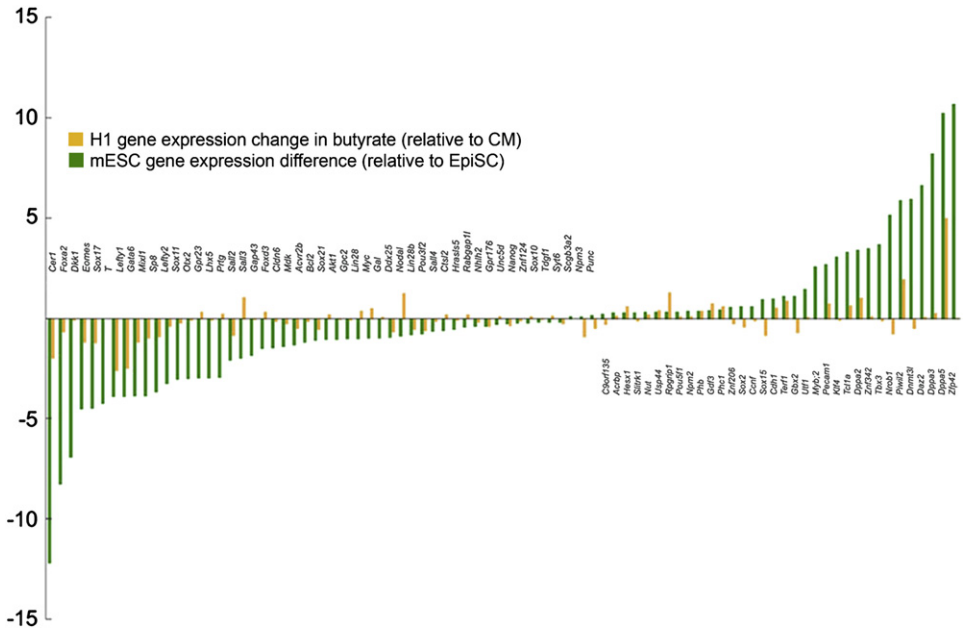

Figure 4. Transcriptional Changes Induced by Butyrate in hESC Correlate with the Relative Abundance of Their Homologues in mESCs Relative to EpiSCs

Differences in expression levels of 87 ESC-related genes between H1 cells cultured in butyrate [H1p48(CM3;B6)] versus CM [H1p48(CM9)] (butyrate/CM, orange bars) and mESC versus EpiSCs (ES/EpiSC, green bars from Tesar et al., 2007). y axis indicates Log 2 fold change. Spearman's rho correlation coefficient for the two data sets is 0.42. $p < 10^{-4}$.

revealed no change in DNA methylation by day 7; however, significant declines were observed on days 14 and 28 (Figure 7C). These kinetics are also consistent with a replication-dependent decline in DNA methylation.

HDACi and ESC Self-Renewal

Other HDACi also supported hESC self-renewal. Trichostatin A (TSA) supported H1 cells for more than 30 passages (Figure S9A), whereas valproic acid (0.5 mM) was effective only in maintaining hESCs previously converted to butyrate culture conditions. Each HDACi induced a subtly different, but reversible, colony morphology, most apparent at the colony edges. Butyrate, butyryl CoA (the retained derivative of butyrate uptake in mitochondria), suberoylanilide hydroxamic acid (vorinostat/SAHA), and TSA-exposed cells plated tightly with sharply demarcated edges, whereas some cell spread at the edges was seen in CM. Stretching of cells at the colony edge was also observed in response to valproic acid. hESC cultured in

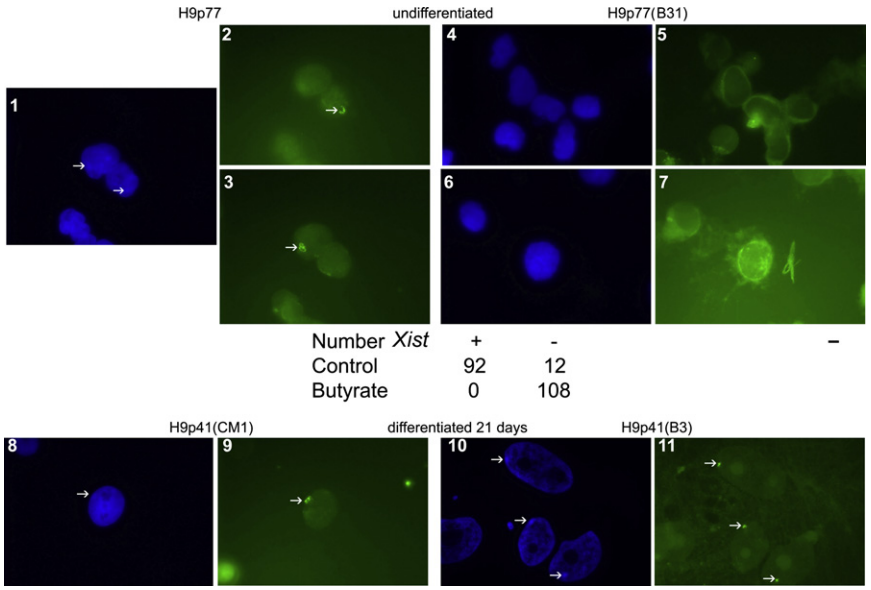

Figure 5. Butyrate Cultures Are Associated with a Lack of *Xist*

Dapi nuclear stain indicating the presumptive presence of the condensed X chromatin (arrows, [1]) and accompanying *Xist* expression (arrows, [2] and [3]) in later passage H9 cells. The same cells grown for the last 31 passages in butyrate on feeders did not show condensation of the X chromatin ([4] and [6]) or *Xist* ([5] and [7]). Below (1)–(7) are the corresponding counts of *Xist*-positive versus -negative cells on the coverslips. Dapi staining of earlier passage H9 cells grown on feeders with one passage in CM shows evidence of X-inactivation upon differentiation for 21 days ([8], Dapi, and [9], *Xist*). Cells grown for three passages in butyrate followed by differentiation for 21 days in the absence of butyrate showed clear evidence of appropriate *Xist* body formation induced by differentiation ([10], Dapi, and [11], *Xist*). Arrows depict location of condensed chromatin (Dapi) and *Xist* bodies (green, *Xist*). The size bar indicates 5 μm.

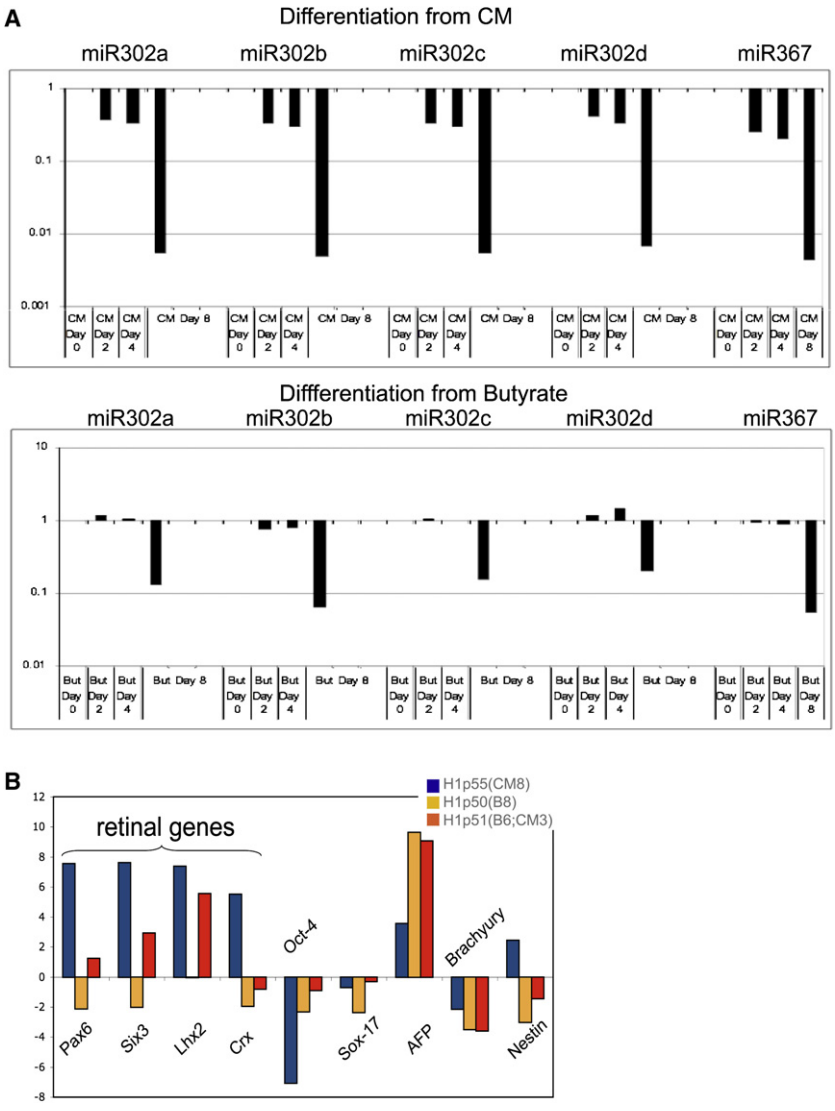

Figure 6. hESCs Cultured in Butyrate Differentiate More Slowly than hESCs Cultured in CM

(A) Time course of 302 family member miRNA expression in H1 cells during an 8 day course of differentiation. Top panels: H1 cells cultured in CM prior to differentiation [H1p69(CM14)]. Bottom panels: H1 cells cultured in butyrate prior to differentiation [H1p67(B15)]. Note that butyrate-treated H1 cells exhibit a slower decline in 302 family miRNAs with differentiation compared to H1 cells cultured in CM.

(B) qRTPCR of differentiation-associated transcripts in H1 cells cultured according to a previously published neuroretinal differentiation protocol (Lamba et al., 2006). Blue bars, H1 cells cultured in CM for eight passages; orange bars, H1 cells cultured in butyrate for eight passages; red bars, H1 cells cultured in butyrate for six passages and reverted to CM for three passages. *Pax6*, *Six3*, *Lhx2*, and *Crx* are associated with retinal differentiation.

TSA or valproic acid divided more rapidly than in butyrate, but not as rapidly as in CM, and were free of lipid-containing vacuoles (data not shown). These findings indicate that as a class, HDACi can promote the self-renewal of ESCs. Suggesting a common mechanism of action, TSA induced a similar, but not identical, transcriptional response in a panel of 18 butyrate responsive genes (Figure S9B). In contrast to butyrate, TSA did not promote improved chimera formation in mice and did not appear to support the long-term maintenance of mESCs without LIF or feeders. We conclude that while not all HDACi share butyrate's full spectrum of activity, HDAC inhibition is at the core of butyrate-induced ESC self-renewal.

DISCUSSION

We show that ESCs can extensively self-renew in response to butyrate, without need for feeder conditioning or recombinant growth factors. ESCs are exquisitely sensitive to butyrate, and self-renewal occurs only within a narrow concentration range, with higher concentrations (prevalent in the literature) inducing differentiation. Since other HDACi (TSA, valproic acid, and vorinostat) also promote ESC self-renewal, our results point to the existence of a core machinery for ESC self-renewal that is under HDAC control and that can be activated upon HDAC inhibition. Nonetheless, we do note differences in the response of ESCs to various HDACi. For example, TSA did not allow mESC to develop appropriately in the embryo to generate chimeras, and valproic acid could only maintain hESCs in culture that had already been converted to butyrate. We cannot discern whether these differences reflect butyrate's potency or range of HDAC inhibition, or additional activities beyond HDAC inhibition. Within cells, butyrate is converted to butyryl CoA, which we show can also support hESC self-renewal. Butyryl CoA is integral to mammalian metabolism both for immediate energy and for energy storage and can be utilized to build triacylglycerols and phospholipids, the likely contents of the oil red O^+ droplets present in butyrate-treated cells.

The transcriptional response to butyrate in hESCs was distinctive, as exemplified by *Dppa5*. Butyrate induced a number of embryonic/cancer/testes-associated genes in hESCs, including *Dppa5* and its neighbors *Ddx43/HAGE* and *Ecat1*. A CpG island upstream of *Dppa5*, unmethylated in sperm and testes, is densely methylated in peripheral blood (Shen et al., 2007) and in hESCs cultured in CM (Figure 7). Butyrate treatment dramatically reduced methylation of this CpG island, providing the first example, to our knowledge, of CpG demethylation in response to an HDACi (Cameron et al., 1999). This demethylation was highly context dependent since other induced genes (*Ddx43*, *Rcn3*, and *Cxcl5*) were only modestly demethylated and *Sp5*, a repressed gene, was moderately hypermethylated in response to butyrate (preliminary observations). Butyrate also prevented the appearance of *Xist* expression in later passage H9 cells,

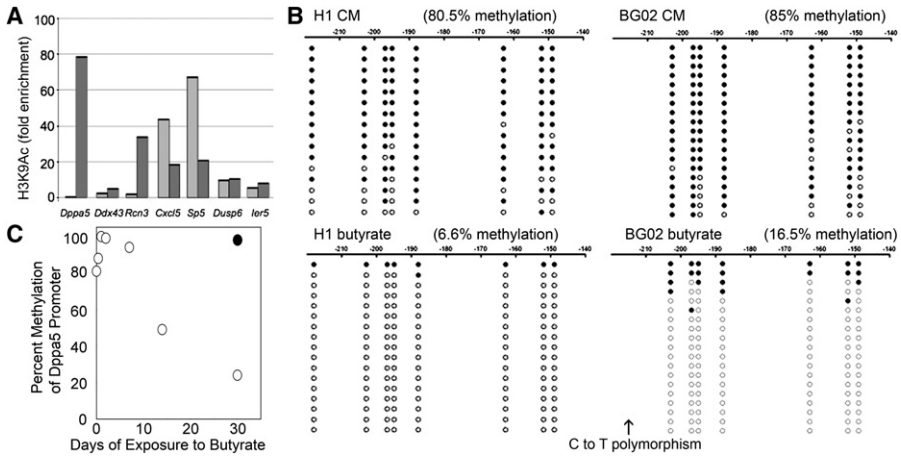

Figure 7. Epigenetic Responses to Butyrate

(A) H3K9 acetylation in the promoters of butyrate-responsive genes. Light gray bars indicate BG02 cells cultured in CM [BG02p74(CM35)]; dark gray bars indicate BG02 cells cultured in butyrate [BG02p79(CM29;B24)]. An antibody directed against total histone H3 provided a control.

(B) Bisulfite sequencing of the *Dppa5* promoter in H1 cells (left) and BG02 cells (right). Closed circles indicate the presence of methylation, and open circles indicate the absence of methylation. Numbers indicate the distance upstream from the transcription start site. Comparisons were made between H1p77(CM43) versus H1p84(B42) (left panels) and BG02p49(CM10) versus BG02p76(CM29;B18) (right panels).

(C) Changes in *Dppa5* promoter methylation at various time points following a switch from CM [H1p63(CM8)] to butyrate. Open circles indicate methylation levels in butyrate-treated cells, whereas the closed circle depicts *Dppa5* promoter methylation in the same cells continuously cultured in CM.

suggesting an inhibitory effect on X inactivation. In general, the induction of butyrate-responsive genes is rapidly reversed following butyrate withdrawal (Davie, 2003). However, another unusual feature of the butyrate response observed here was the very gradual return of a subset of butyrate-regulated genes back to baseline after reverting hESCs back to CM (Figure 3B; Figure S6C; Table S4). This slow return to baseline demonstrates the existence of a mechanism for the prolonged transcriptional memory of butyrate exposure.

The most surprising finding from our study was the contrast between butyrate's ability to support ESC self-renewal across species, while eliciting virtually nonoverlapping transcriptional responses in hESCs versus mESCs. Our gene expression analysis strongly supports the conclusion that HDACi push mESCs forward and pull hESCs backward toward a developmental corollary intermediate between ESCs and EpiSCs. Other reports support the existence of alternative ESC-like states. Culturing mESCs in medium conditioned by HepG2 cells was found to elicit a gene expression profile similar to early primitive ectoderm, with induction of *Fgf5* and repression of *Rex1*, *Stella/Dppa3*, and *Pecam1* (Rathjen et al., 1999). These early primitive ectoderm-like (EPL) cells could not form chimeric mice yet reverted back to an ESC-like state (regaining chimera-forming ability) upon return to LIF. Very recently, another group used a GFP reporter under control of a *Stella/Dppa3* promoter to identify large numbers of STELLA-negative, PECAM1-negative ESCs in LIF-containing cultures (Hayashi et al., 2008). While chimera-forming ability was not tested, the STELLA-negative population reverted to more of an ESC-like state when cultured in the presence of feeders or TSA. In contrast to these published reports, the alternative ESC state induced by butyrate appears to be better able to generate chimeric mice. While butyrate might also enhance the poor chimera-forming ability of EpiSCs, it does not convert EpiSCs to mESCs, consistent with the notion that EpiSCs fall beyond the range of interconvertible ESC states (Hayashi et al., 2008).

Whether the effects described here have a corollary in vivo is not known. A potential physiological underpinning is suggested by the conservation of butyrate responsiveness from mouse to human ESCs and mEpiSCs. Our data suggest that butyrate may fine-tune peri-implantation development. That butyrate-treated mouse ESCs retain the ability to contribute to chimeric mice, including transmission to the germline, indicates that butyrate effects are fully reversible and exert no obvious harm on embryonic development. Butyrate exposure improves the ability of previously unsuccessful mESC clones to generate chimeras; thus, butyrate confers an ability to survive and contribute appropriately in the context of the blastocyst. That these mESC clones, in the absence of butyrate, are unable to generate chimeras (although pups are born) suggests that they do not integrate or participate in normal development and can only respond appropriately with the assistance of butyrate.

Our results demonstrate that butyrate and other HDACi can shape the ESC state. Cross-species convergence toward a common ESC state raises the possibility of an as yet undiscovered physiological signaling axis that involves butyrate or analogous molecules that can potently regulate development.

EXPERIMENTAL PROCEDURES

hESC Culture

Initial cultures of hESC (H1 [NIH code WA01], H7 [WA07], H9 [WA09], H13 [WA13], hSF6 [UC06], BG02, and BG03) and nonhuman primate (rh366.4) ESCs were grown on a feeder layer of γ-irradiated (3000 rads) primary mouse embryonic fibroblasts (MEF) (Abbondanzo et al., 1993). For cultures without feeders, cells were plated on Matrigel (BD Biosciences) diluted according to manufacturer's instructions. Human ESC culture medium (hESM) consisted of DMEM/F12-containing GlutaMax supplemented with 20% serum replacer (SR), 1 mM sodium pyruvate, 0.1 mM nonessential amino acids, 50 U/ml

penicillin, 50 mg/ml streptomycin, (all from Invitrogen, Carlsbad, CA), and 0.1 mM β-mercaptoethanol (Sigma, St. Louis, MO). Conditioned medium (CM) was made by incubating hESM in the presence of MEF as described in the Supplemental Experimental Procedures. CM also included 2 ng/ml basic FGF (FGF2, Peprotech, Rocky Hill, NJ, USA). hESCs cultured in the presence of 0.2 to 0.3 mM sodium butyrate (Sigma) were cultured in hESM in the absence of MEF conditioning or FGF2. Concentrations of other HDACi were 10 nM TSA, 0.5 mM valproic acid, 10 μM butyryl CoA (all from Sigma), and 400 nM vorinostat (Cayman Chemical, Ann Arbor, MI). Nomenclature for culture conditions follows the following convention: cell line, total passage number (number of passages off of feeders, where CM indicates culture on Matrigel in conditioned medium and B indicates culture in butyrate—generally on Matrigel with no feeder or added FGF—followed by the number of passages under a different growth medium, etc.). Thus, H1p62(CM4;B6;CM3) would be H1 grown for 62 passages overall. Of the last 13 passages, all were on Matrigel without feeders, and passages 49–52 were in CM, passages 53–59 were in butyrate, and passages 60–62 were in CM. Occasionally, hESCs were cultured in butyrate on MEFs. When this was done, it is listed in the text.

mESC Culture

mESCs were cultured in the same medium described for hESC, except the serum replacer in human medium was substituted with 20% FBS (ES Cell Qualified, Invitrogen). MEF: free cultures were performed on gelatin-coated dishes using medium supplemented with 1000 units/ml mouse LIF (ESGRO, Chemicon) or butyrate (0.2 mM). On occasion, butyrate was added to mESC cultured on MEF. Cultures of LIF receptor null mESCs (a gift from Austin Smith), gp130 null mESCs (a gift from Ian Chambers), and derivation of mESCs were performed as described in the Supplemental Experimental Procedures.

mEpiSC Culture

Mouse EpiSC line no. 5 (a gift from Paul Tesar and Ron McKay) was cultured as described (Tesar et al., 2007). In addition, new mEpiSC lines were derived as previously described (Tesar et al., 2007).

Immunohistochemistry and Flow Cytometry

Maintenance of an undifferentiated phenotype was established by immunohistochemistry using antibodies for Oct-4 (R&D Systems; 1:200 dilution) and SSEA-4 (Chemicon; 1:50 dilution) and by staining for alkaline phosphatase (AP) activity using a Black Alkaline Phosphatase Substrate Kit II (Vector Laboratories). Flow cytometry was performed using a FACScan flow cytometer and Cell Quest software (BD Biosciences) and the following antibodies: anti-SSEA4, anti-TRA-1-60 and TRA-1-81 (Chemicon), and anti-SSEA-3 (R&D Systems). For cell-cycle analysis, cells were harvested, washed with phosphate-buffered saline (PBS), and fixed in 70% ethanol. Fixed cells were stained with propidium iodide (PI), and DNA content was measured by the intensity of the fluorescence produced by PI. Data were analyzed with the Modfit 3.0 software (Verity House Software).

Quantitative PCR

Total RNA was purified using the RNeasy Micro Kit (QIAGEN) following the manufacturer-specified protocol. Reverse transcription of total RNA was performed using random hexamers with the SuperScript III First-Strand Synthesis System for RT-PCR (Invitrogen). Quantitative PCR was performed in triplicate using TaqMan Universal PCR Master Mix, No AmpErase UNG (Applied Biosystems), or SYBR Green PCR Master Mix (Applied Biosystems) in 25 μl reactions in an Applied Biosystems 7900HT Fast Real-Time PCR System. Settings and primer sequences are described in the Supplemental Experimental Procedures.

Microarray Analysis

Agilent whole-human genome arrays were hybridized with total RNA from H1 cells cultured in each of the following conditions (2 arrays per condition): (1) Cultured on Matrigel on CM; (2) cultured for 6 passages in butyrate; (3) cultured for 3 passages in butyrate, followed by 3 passages in CM. Group 1 was compared to 2 in independent triplicate, and 2 was compared to 3 in independent triplicate. Thus, by experimental design and Agilent platform, Groups 1 and 3 served as controls relative to 2. Agilent whole-mouse genome microarrays were hybridized with total RNA from R1 cells cultured on gelatin without feeder support in LIF or R1 cells cultured in 0.2 mM butyrate without LIF or feeder support. These were run in independent quadruplicate.

Genes were defined as differentially expressed if they showed both a change in expression at a false discovery rate of 0.2 as analyzed by an empirical paired t test and a 1.5-fold change in expression level. Genes were matched across the mouse and human data sets using Homologene. See the Supplemental Experimental Procedures for more details.

Bisulfite-Sequencing Analysis of Promoter Methylation and Chromatin Immunopreciptation Analysis of Promoter Acetylation

Bisulfite-sequencing to assess *Dppa5* promoter methylation was performed as reported previously (Shen et al., 2007). Chromatin immunoprecipitation (ChIP) analysis to assess promoter acetylation was performed as described (Nelson et al., 2006) and utilized an anti-acetyl-histone H3 antibody, which recognizes lysine residues 9 and 14 (Millipore).

ACCESSION NUMBERS

The data discussed in this publication have been deposited in NCBI's Gene Expression Omnibus (Edgar et al., 2002) and are accessible through GEO Series accession number GSE15112 (http://www.ncbi.nlm.nih.gov/projects/geo/query/acc.cgi?acc=GSE15112). Additional information from our microarray analysis is available at https://depts.washington.edu/iscrm/GS_data/gsdata.html.

SUPPLEMENTAL DATA

The Supplemental Data include nine figures, four tables, Supplemental Experimental Procedures, and Supplemental References and can be found with this article online at http://www.cell.com/cell-stem-cell/supplemental/S1934-5909(09)00102-7.

ACKNOWLEDGMENTS

We thank Daniel G. Miller, William Noble, Richard Young, Matt Guenther, Paul Tesar, Ron McKay, Piper Treuting, Edith Wang, and Julian Simon for useful discussions. We thank Austin Smith for LIFR$^{-/-}$ mESCs and Ian Chambers for gp130$^{-/-}$ mESCs; Paul Tesar and Ron McKay for mEpiSCs; Samuel Sun for assistance with data analysis; and Jeff Okada, Jennifer Potter, Chris Cavanaugh, and Jennifer Hesson for technical support. We also thank Robert Hall at the University of Washington Center for Array Technologies and William Howald at the Mass Spectrometry Center for their expertise and assistance. This work was supported by NIH grant 1P01GM081619 and through the Institute for Stem Cell and Regenerative Medicine (ISCRM) of the University of Washington. P.P. is supported by a Michael Smith Foundation for Health Research Career Investigator Award and NIH grant GM076990. C.B.W. made the initial observation regarding butyrate's activity in culture, designed and performed experiments, interpreted findings, prepared figures, and helped to draft and revise the manuscript; L.W. performed all experiments pertaining to flow cytometry and assisted with many of the qPCR studies; B.M., R.L., and P.P. analyzed data from expression arrays of mESCs and hESCs and compared them to published expression arrays; R.F. designed and performed chromatin immunoprecipitation analyses; A.M.N. assisted C.B.W. in many of the culture studies of mESC and hESC, as well as in generating mESC lines in the presence of butyrate; D.D. and B.B. designed and performed a number of qPCR experiments; M.B. and M.T. performed qPCR for microRNAs; S.M.G. performed studies of *Xist* expression and critically reviewed the manuscript; L.S. and J.-P.I. performed promoter methylation analysis; B.A. explored metabolic fate of cells grown in butyrate; D.L. tested directed differentiation to a neuroretinal fate; Z-J.D. performed telomerase assays and assisted in study design and in revising the manuscript; and C.A.B. assisted in designing experiments, interpreting results, preparing figures, and writing the manuscript.

Received: April 15, 2008
Revised: November 12, 2008
Accepted: March 6, 2009
Published: April 2, 2009

REFERENCES

Abbondanzo, S.J., Gadi, I., and Stewart, C.L. (1993). Derivation of embryonic stem cell lines. Methods Enzymol. *225*, 803–823.

Andäng, M., Hierling-Leffler, J., Moliner, A., Lundgren, T.K., Castelo-Branco, G., Nanou, E., Pozas, E., Brvia, V., Halliez, S., Nishimaru, H., et al. (2008). Histone H2AX-dependent GABA(A) receptor regulation of stem cell proliferation. Nature *451*, 460–464.

Baker, D.E., Harrison, N.J., Maltby, E., Smith, K., Moore, H.D., Shaw, P.J., Heath, P.R., Holden, H., and Andrews, P.W. (2007). Adaptation to culture of human embryonic stem cells and oncogenesis in vivo. Nat. Biotechnol. *25*, 207–215.

Becker, K.A., Stein, J.L., Lian, J.B., van Wijnen, A.J., and Stein, G.S. (2007). Establishment of histone gene regulation and cell cycle checkpoint control in human embryonic stem cells. J. Cell. Physiol. *210*, 517–526.

Ben-Porath, I., Thomson, M.W., Carey, V.J., Ge, R., Bell, G.W., Regev, A., and Weinberg, R.A. (2008). An embryonic stem cell-like gene expression signature in poorly differentiated aggressive human tumors. Nat. Genet. *40*, 499–507.

Bernstein, B.E., Mikkelsen, T.S., Xie, X., Kamal, M., Huebert, D.J., Cuff, J., Fry, B., Meissner, A., Wernig, M., Plath, K., et al. (2006). A bivalent chromatin structure marks key developmental genes in embryonic stem cells. Cell *125*, 315–326.

Boffa, L.C., Vidali, G., Mann, R.S., and Allfrey, V.G. (1978). Suppression of histone deacetylation in vivo and in vitro by sodium butyrate. J. Biol. Chem. *253*, 3364–3366.

Brons, I.G., Smithers, L.E., Trotter, M.W., Rugg-Gunn, P., Sun, B., Chuva de Sousa Lopes, S.M., Howlett, S.K., Clarkson, A., Ahrlund-Richter, L., Pedersen, R.A., and Vallier, L. (2007). Derivation of pluripotent epiblast stem cells from mammalian embryos. Nature *448*, 191–195.

Buszczak, M., and Spradling, A.C. (2006). Searching chromatin for stem cell identity. Cell *125*, 233–236.

Cameron, E.E., Bachman, K.E., Myöhänen, S., Herman, J.G., and Baylin, S.B. (1999). Synergy of demethylation and histone deacetylase inhibition in the re-expression of genes silenced in cancer. Nat. Genet. *21*, 103–107.

Chambers, I., Silva, J., Colby, D., Nichols, J., Nijmeijer, B., Robertson, M., Vrana, J., Jones, K., Grotewold, L., and Smith, A. (2007). Nanog safeguards pluripotency and mediates germline development. Nature *450*, 1230–1234.

Dahéron, L., Opitz, S.L., Zaehres, H., Lensch, M.S., Andrews, P.W., Itskovitz-Eldor, J., and Daley, G.Q. (2004). LIF/STAT3 signaling fails to maintain self-renewal of human embryonic stem cells. Stem Cells *22*, 770–778.

Davie, J.R. (2003). Inhibition of histone deacetylase activity by butyrate. J. Nutr. *133*, 2485S–2493S.

Denning, C., Allegrucci, C., Priddle, H., Barbadillo-Muñoz, M.D., Anderson, D., Self, T., Smith, N.M., Parkin, C.T., and Young, L.E. (2006). Common culture conditions for maintenance and cardiomyocyte differentiation of the human embryonic stem cell lines, BG01 and HUES-7. Int. J. Dev. Biol. *50*, 27–37.

Dreesen, O., and Brivanlou, A.H. (2007). Signaling pathways in cancer and embryonic stem cells. Stem Cell Rev. *3*, 7–17.

Edgar, R., Domrachev, M., and Lash, A.E. (2002). Gene Expression Omnibus: NCBI gene expression and hybridization array data repository. Nucleic Acids Res. *30*, 207–210.

Eiselleova, L., Peterkiva, I., Neradil, J., Slaninova, I., Hampl, A., and Dvorak, P. (2008). Comparative study of mouse and human feeder cells for human embryonic stem cells. Int. J. Dev. Biol. *52*, 353–363.

Hall, L.L., Byron, M., Butler, J., Becker, K.A., Nelson, A., Amit, M., Itskovitz-Eldor, J., Stein, J., Stein, G., Ware, C., and Lawrence, J.B. (2008). X-inactivation reveals epigenetic anomalies in most hESC but identifies sublines that initiate as expected. J. Cell. Physiol. *6*, 445–452.

Hayashi, K., Chuva de Sousa Lopes, S.M., Tang, F., and Surani, M.A. (2008). Dynammic equilibrium and heterogeneity of mouse pluripotent stem cells with distinct functional and epigenetic states. Cell Stem Cell *3*, 391–401.

Huangfu, D., Osafune, K., Maehr, R., Guo, W., Eijkelenboom, A., Chen, S., Muhlestein, W., and Melton, D.A. (2008). Induction of pluripotent stem cells from primary human fibroblasts with only Oct4 and Sox2. Nat. Biotechnol. *26*, 1269–1275.

International Stem Cell Initiative, Adewumi, O., Aflatoonian, B., Ahrlund-Richter, L., Amit, M., Andrews, P.W., Beighton, G., Bello, P.A., Benvenisty, N., Berry, L.S., et al. (2007). Characterization of human embryonic stem cell lines by the International Stem Cell Initiative. Nat. Biotechnol. *25*, 803–816.

Ivanova, N., Dobrin, R., Lu, R., Kotenko, I., Levorse, J., DeCoste, C., Schafer, X., Lun, Y., and Lemischka, I.R. (2006). Dissecting self-renewal in stem cells with RNA interference. Nature *442*, 533–538.

Kaji, K., Nichols, J., and Hendrich, B. (2007). Mbd3, a component of the NuRD co-repressor complex, is required for development of pluripotent cells. Development *134*, 1123–1132.

Lamba, D.A., Karl, M.O., Ware, C.B., and Reh, T.A. (2006). Efficient generation of retinal progenitor cells from human embryonic stem cells. Proc. Natl. Acad. Sci. USA *103*, 12769–12774.

Levenstein, M.E., Ludwig, T.E., Xu, R.H., Llanas, R.A., VanDenHeuvel-Kramer, K., Manning, D., and Thomson, J.A. (2006). Basic fibroblast growth factor support of human embryonic stem cell self-renewal. Stem Cells *24*, 568–574.

Li, C.M., Kim, C.E., Margolin, A.A., Guo, M., Zhu, J., Mason, J.M., Hensle, T.W., Murty, V.V., Grundy, P.E., Fearon, E.R., et al. (2004). CTNNB1 mutations and overexpression of Wnt/beta-catenin target genes in WT1-mutant Wilms' tumors. Am. J. Pathol. *165*, 1943–1953.

Nakagawa, M., Koyanagi, M., Tanabe, K., Takahashi, K., Ichisaka, T., Aoi, T., Okita, K., Mochiduki, Y., Takizawa, N., and Yamanaka, S. (2007). Generation of induced pluripotent stem cells without Myc from mouse and human fibroblasts. Nat. Biotechnol. *26*, 101–106.

Nelson, J.D., Denisenko, O., and Bomsztyk, K. (2006). Protocol for the fast chromatin immunoprecipitation (ChIP) method. Nat. Protocols *1*, 179–185.

Park, I.H., Zhao, R., West, J.A., Yabuuchi, A., Huo, H., Ince, T.A., Lerou, P.H., Lensch, M.W., and Daley, G.Q. (2007). Reprogramming of human somatic cells to pluripotency with defined factors. Nature *451*, 135–136.

Pereira, L., Yi, F., and Merrill, B.J. (2006). Repression of Nanog Gene Transcription by Tcf3 Limits Embryonic Stem Cell Self-Renewal. Mol. Cell. Biol. *26*, 7479–7491.

Rada-Iglesias, A., Enroth, S., Ameur, A., Koch, C.M., Clelland, G.K., Respuela-Alonso, P., Wilcox, S., Dovey, O.M., Ellis, P.D., Langford, C.F., et al. (2007). Butyrate mediates decrease of histone acetylation centered on transcription start sites and down-regulation of associated genes. Genome Res. *17*, 708–719.

Rathjen, J., Lake, J.A., Bettess, M.D., Washington, J.M., Chapman, G., and Rathjen, P.D. (1999). Formation of a primitive ectoderm like cell population, EPL cells, from ES cells in response to biologically derived factors. J. Cell Sci. *112*, 601–612.

Savatier, P., Huang, S., Szekely, L., Wiman, K.G., and Samarut, J. (1994). Contrasting patterns of retinoblastoma protein expression in mouse embryonic stem cells and embryonic fibroblasts. Oncogene *9*, 809–818.

Shen, L., Kondo, Y., Guo, Y., Zhang, J., Zhang, L., Ahmend, S., Shu, J., Chen, X., Waterland, R.A., and Issa, J.P. (2007). Genome-wide profiling of DNA methylation reveals a class of normally methylated CpG island promoters. PLoS Genet. *3*, 2023–2036. 10.1371/journal.pgen.0030181.

Smith, A.G. (2001). Embryo-derived stem cells: of mice and men. Annu. Rev. Cell Dev. Biol. *17*, 435–462.

Stewart, C.L., Kaspar, P., Brunet, L.J., Bhatt, H., Gadi, I., Köntgen, F., and Abbondanzo, S.J. (1992). Blastocyst implantation depends on maternal expression of leukaemia inhibitory factor. Nature *359*, 76–79.

Tabibzadeh, S., and Hemmati-Brivanlou, A. (2006). Lefty at the crossroads of "stemness" and differentiative events. Stem Cells *24*, 1998–2006.

Takahashi, K., and Yamanaka, S. (2006). Induction of pluripotent stem cells from mouse embryonic and adult fibroblast cultures by defined factors. Cell *126*, 663–676.

Takahashi, K., Tanabe, K., Ohnuki, M., Narita, M., Ichisaka, T., Tomoda, K., and Yamanaka, S. (2007). Induction of pluripotent stem cells from adult human fibroblasts by defined factors. Cell *131*, 861–872.

Tesar, P.J., Chenoweth, J.G., Brook, F.A., Davies, T.J., Evans, E.P., Mack, D.L., Gardner, R.L., and McKay, R.D. (2007). New cell lines from mouse epiblast share defining features with human embryonic stem cells. Nature *448*, 196–199.

Thomson, J.A., Itskovitz-Eldor, J., Shapiro, S.S., Waknitz, M.A., Swiergiel, J.J., Marshall, V.S., and Jones, J.M. (1998). Embryonic stem cell lines derived from human blastocysts. Science *282*, 1145–1147.

Vallier, L., Alexander, M., and Pedersen, R.A. (2005). Activin/Nodal and FGF pathways cooperate to maintain pluripotency of human embryonic stem cells. J. Cell Sci. *118*, 4495–4509.

Ware, C.B., Horowitz, M.C., Renshaw, B.R., Hunt, J.S., Liggitt, D., Koblar, S.A., Gliniak, B.C., McKenna, H.J., Papayannopoulou, T., Thoma, B., et al. (1995). Targeted disruption of the low-affinity leukemia inhibitory factor receptor gene causes placental, skeletal, neural and metabolic defects and results in perinatal death. Development *121*, 1283–1299.

Ware, C.B., Nelson, A.M., and Blau, C.A. (2006). A comparison of NIH-approved human ESC lines. Stem Cells *24*, 2677–2684.

Weidinger, G., Thorpe, C.J., Wuennenberg-Stapleton, K., Ngai, J., and Moon, R.T. (2000). The Sp1-related transcription factors Sp5 and Sp5-like act downstream of Wnt/beta-catenin signaling in mesoderm and neuroectoderm patterning. Curr. Biol. *15*, 489–500.

Willert, J., Epping, M., Pollack, J.R., Brown, P.O., and Nusse, R.A. (2002). transcriptional response to Wnt protein in human embryonic carcinoma cells. BMC Dev. Biol. *2*, 8.

Wong, D.J., Liu, H., Ridky, T.W., Cassarino, D., Segal, E., and Chang, H.Y. (2008). Module map of stem cell genes guides creation of epithelial cancer stem cells. Cell Stem Cell *2*, 333–344.

Xiao, L., Yuan, X., and Sharkis, S.J. (2006). Activin A maintains self-renewal and regulates fibroblast growth factor, Wnt, and bone morphogenic protein pathways in human embryonic stem cells. Stem Cells *24*, 1476–1486.

Xu, W.S., Parmigiani, R.B., and Marks, P.A. (2007). Histone deacetylase inhibitors: molecular mechanisms of action. Oncogene *26*, 5541–5552.

Yao, H.H., Matzuk, M.M., Jorgez, C.J., Menke, D.B., Page, D.C., Swain, A., and Capel, B. (2004). Follistatin operates downstream of Wnt4 in mammalian ovary organogenesis. Dev. Dyn. *230*, 210–215.

Yi, F., Pereira, L., and Merrill, B.J. (2008). Tcf3 functions as a steady-state limiter of transcriptional programs of mouse embryonic stem cell self-renewal. Stem Cells *26*, 1951–1960.

Ying, Q.L., Wray, J., Nichols, J., Batlle-Morera, L., Doble, B., Woodgett, J., Cohen, P., and Smith, A. (2008). The ground state of embryonic stem cell self-renewal. Nature *453*, 519–523.

Yu, J., Vodyanik, M.A., Smuga-Otto, K., Antosiewicz-Bourget, J., Frane, J.L., Tian, S., Nie, J., Jonsdottir, G.A., Ruotti, V., Stewart, R., et al. (2007). Induced Pluripotent Stem Cell Lines Derived from Human Somatic Cells. Science *318*, 1917–1920.

Zirn, B., Samans, B., Wittmann, S., Pietsch, T., Leuschner, I., Graf, N., and Gessler, M. (2006). Target genes of the WNT/beta-catenin pathway in Wilms tumors. Genes Chromosomes Cancer *45*, 565–574.